


## Research Article

# Structural Characterization and Immunomodulatory Activity of Polysaccharides from *Polygonatum sibiricum* Prepared with Deep Eutectic Solvents

Jikun Meng,<sup>1</sup> Chunbo Guan,<sup>1</sup> Qiufeng Chen,<sup>1</sup> Xiao Pang,<sup>1</sup> Heqin Wang,<sup>1</sup> Xinwen Cui,<sup>1</sup> Ran Ye,<sup>2</sup> and Xiuqing Zhang<sup>1</sup> 

<sup>1</sup>College of Food Science and Nutritional Engineering, China Agricultural University, Beijing 100083, China

<sup>2</sup>Beijing Yuanmai Shanqiu Food Co., Ltd., Beijing 102200, China

Correspondence should be addressed to Xiuqing Zhang; [xiuqingzhang@cau.edu.cn](mailto:xiuqingzhang@cau.edu.cn)

Received 19 April 2023; Revised 3 July 2023; Accepted 7 July 2023; Published 24 August 2023

Academic Editor: Seyed Mohammad Taghi Gharibzahedi

Copyright © 2023 Jikun Meng et al. This is an open access article distributed under the Creative Commons Attribution License, which permits unrestricted use, distribution, and reproduction in any medium, provided the original work is properly cited.

Deep eutectic solvents (DES), as a new, efficient, and green solvents, have attracted more attention in recent years. This study was performed to extract *Polygonatum sibiricum* polysaccharides using DES (DPSP). Subsequently, DPSP was subjected to DEAE-Sephadex Fast Flow and Sephadex G-100 column for further purification (DPSP-3). Structural characterization and immunomodulatory activity in RAW264.7 cells were performed. Results showed that the yield of DPSP was  $(15.62 \pm 0.71)\%$ , and its yield was 1.53 times that of the polysaccharides extracted using the pharmacopoeia method (PSP). DPSP-3 had a smaller molecular weight ( $3.2 \times 10^6$  Da) and a higher ratio of galactose (65.75%) and mannose (19.76%) as compared to PSP. The scanning electron microscope (SEM) showed that DPSP-3 had curly shape, lamellar surface, and a few spherical edges, which were significantly different from PSP and DPSP. Both PSP and DPSP-3 could significantly improve phagotrophic capacity and increase the release of ROS, NO, IL-6, and TNF- $\alpha$  in RAW 264.7 cells, and DPSP-3 had better immunomodulatory activity. In summary, compared to the pharmacopoeia method, polysaccharides prepared using the DES extraction method showed higher yield and improved immunomodulatory activity.

## 1. Introduction

Polysaccharides are commonly extracted by using the pharmacopoeia or the acid (alkali) extraction methods, which are assisted by ultrasound, microwaves, and enzymes. However, there are some inherent limitations in these methods, such as high energy consumption, long extraction time, low extraction efficiency, and poor selectivity [1]. Traditional solvents (hot water, acid, and alkali) extract functional components in natural plants though destroying cell walls. However, ionic liquids can dissolve plant cell walls to release functional components from cells, so as to achieve the goal of improving the extraction ratio. Deep eutectic solvents (DES) is also considered to be ionic liquids, which

has more excellent properties than other ionic liquids, such as lower cost, easy to prepare and store, inexpensive, biodegradability, and safety, as well as sustainability [2, 3]. DES is a mixture of hydrogen acceptor and hydrogen donor heated and dissolved proportionately, which remains uniform and transparent at room temperature [4]. The most widespread hydrogen acceptor is choline chloride (CC), yet the selection of hydrogen donors is diversified, including oxalic acid, glucose, sucrose, lactic acid, ethylene glycol etc. [5, 6]. Among them, oxalic acid is relatively safe in food processing. Meanwhile, studies showed that the yield of polysaccharides using DES (CC/oxalic acid) as a solvent was higher than that of using other types of DES, which might be due to its stronger hydrogen bonding ability and

electrostatic interactions with polysaccharides [7, 8]. At present, DES has been successfully used to extract natural product, such as polysaccharides [9], flavonoids [10], proteins [11], and nicotinic acid [12].

*Polygonatum sibiricum*, also known as Jitou ginger, is widely cultivated in China [13]. In Traditional Chinese Medicine, *P. sibiricum* is known for improving vital energy, nourishing the heart and lungs, and strengthening the muscles and bones [14]. Studies showed that *P. sibiricum* mainly contained polysaccharides, saponins, flavonoids, and other chemical components, while polysaccharides were one of the main active compounds [3, 15]. *Polygonatum sibiricum* polysaccharides perform antioxidant, antiaging, and immunomodulatory activity, and they also regulate glucose and lipid metabolism [16–19].

Polysaccharides can regulate immunomodulatory activity by enhancing the function of macrophages [20]. Wu found that polysaccharides from Guapian tea leaves (LGP-1) could significantly stimulate the phagocytosis of macrophages, promote NO generation, and trigger TNF- $\alpha$ , IL-6, and IL-1 $\beta$  release dose-dependently. LGP-1 enhanced macrophage immunity via PI3K/AKT and NF- $\kappa$ B signaling pathways, and TLR4 was involved in the process [21]. *Polygala tenuifolia* willd. polysaccharides could promote cell proliferation, increase the secretions of TNF- $\alpha$ , IL-6, and IL-1 $\beta$ , upregulate the expressions of P-p38, P-ERK, and P-JNK, activate macrophages, and exert immune activity by activating MAPKs mediated pathway [22]. This study analyzed the structural characterization of *P. sibiricum* polysaccharides and investigated their immunomodulatory activity in RAW 264.7 cells.

## 2. Materials and Methods

**2.1. Materials.** The dried rhizome of *P. sibiricum* was purchased from Liaoning Wanjia Medical Technology Co., Ltd. (Shenyang, China). DEAE-Sepharose Fast Flow and Sephadex G-100 were purchased from Yuanye Bio-Technology Co., Ltd. (Shanghai, China). Standard dextrans of different molecular weights (6.2 kDa, 10 kDa, 48.8 kDa, 70 kDa, 200 kDa, and 736 kDa) were purchased from Solarbio Science & Technology Co., Ltd. (Beijing, China). Monosaccharide standards (arabinose, fucose, galactose, glucose, glucuronic acid, galacturonic acid, mannose, N-acetyl-d-galactosamine, N-acetyl-d-glucosamine, ribose, rhamnose, and xylose) were purchased from Sigma Chemical Co., Ltd. (St. Louis, MO, USA). Murine macrophage cell line RAW 264.7 was purchased from the Chinese Academy of Sciences (Beijing, China). Dulbecco's modified Eagle's medium (DMEM), fetal bovine serum (FBS), insulin, penicillin, and streptomycin were purchased from GIBCO (Carlsbad, CA, USA). Lipopolysaccharides (LPS), CCK-8 kit, neutral red, and phosphate buffered saline (PBS) were purchased from Solarbio Science & Technology Co., Ltd. (Beijing, China). NO assay kit and ROS assay kit were purchased from Jiancheng Bioengineering Institute (Nanjing, China). IL-6 and TNF- $\alpha$  ELISA kits were purchased from Enzyme-linked Biotechnology Co., Ltd.

(Shanghai, China). All other chemicals and reagents used were of analytical grade.

**2.2. Preparation and Purification of Polysaccharides.** The dried rhizome of *P. sibiricum* was sliced and crushed with a pulverizer (BJ-800A; Deqing Baijie Electric Appliance Co., Ltd, Huzhou, China), which was then passed through a 0.42 mm (60 mesh) sieve to obtain the dried *P. sibiricum* powder. In Figure 1, the powder was immersed in 80% ethanol at room temperature with the ratio of 1 : 50 (m/v) for 30 min. The solution was centrifuged at 6,000 rpm for 10 min to remove lipophilic compounds, and the precipitate was collected for subsequent experience.

The pharmacopoeia method (National Pharmacopoeia Commission, 2020) was used as a comparison. In brief, the obtained precipitate was extracted with deionized water (1 : 50, g/mL) at 100°C for 2 h. The supernatant was combined and concentrated using a rotary evaporator (RE-52AA, Shanghai Yarong Biochemical Instrument Factory, Shanghai, China), the concentrated solution precipitated with 80% ethanol and stored at 4°C for 12 h, and then the obtained precipitate was collected by centrifugation and freeze-dried. Subsequently, the protein was removed by the Sevage reagent (chloroform:n-butanol = 4:1, v/v), and the pigment was removed by the AB-8 macroporous resin column (3.5 cm  $\times$  20 cm). Finally, the product was lyophilized to obtain the crude polysaccharides PSP.

In the DES extraction method [20], 1 g of obtained precipitate was extracted with 20 mL of DES (choline chloride: oxalic acid = 1 : 1, mass ratio) at 70°C for 40 min. After centrifugation (7,000 rpm, 8 min), the obtained supernatant was collected, precipitated with alcohol, deproteinized, and removed pigments, as stated by the pharmacopoeia method above. The obtained polysaccharides were named as DPSP. DPSP was dissolved in deionized water (5 mg/mL). The solution was loaded onto a DEAE-Sepharose Fast Flow column (3.5 cm  $\times$  20 cm), and the column was sequentially eluted with ultrapure water and 0.1, 0.2, 0.4, and 0.6 M sodium chloride (NaCl) solution at a flow rate of 1.0 mL/min. The eluted fractions were collected (5 mL/tube) and monitored. Then, the eluted fraction (0.04 M NaCl aqueous solutions) was concentrated, dialyzed with deionized water for 48 h at 4°C, and freeze-dried to obtain the purified polysaccharides DPSP-3. DPSP-3 (5 mg/mL) was further purified with Sephadex G-200 column (3.5 cm  $\times$  60 cm). Briefly, DPSP-3 was dissolved in ultrapure water (5 mg/mL) and eluted with ultrapure water at a flow rate of 0.5 mL/min. After freeze-drying, the powder obtained was DPSP-3 fraction. The total polysaccharides content in each tube was determined by the phenol-sulfuric acid method.

### 2.3. Structural Characterization Analysis

**2.3.1. Molecular Weight Determination.** 1 mg of sample was dissolved in 1 mL of ultrapure water and filtered and measured by high pressure gel permeation chromatography (HPGPC). The chromatographic conditions were HPLC

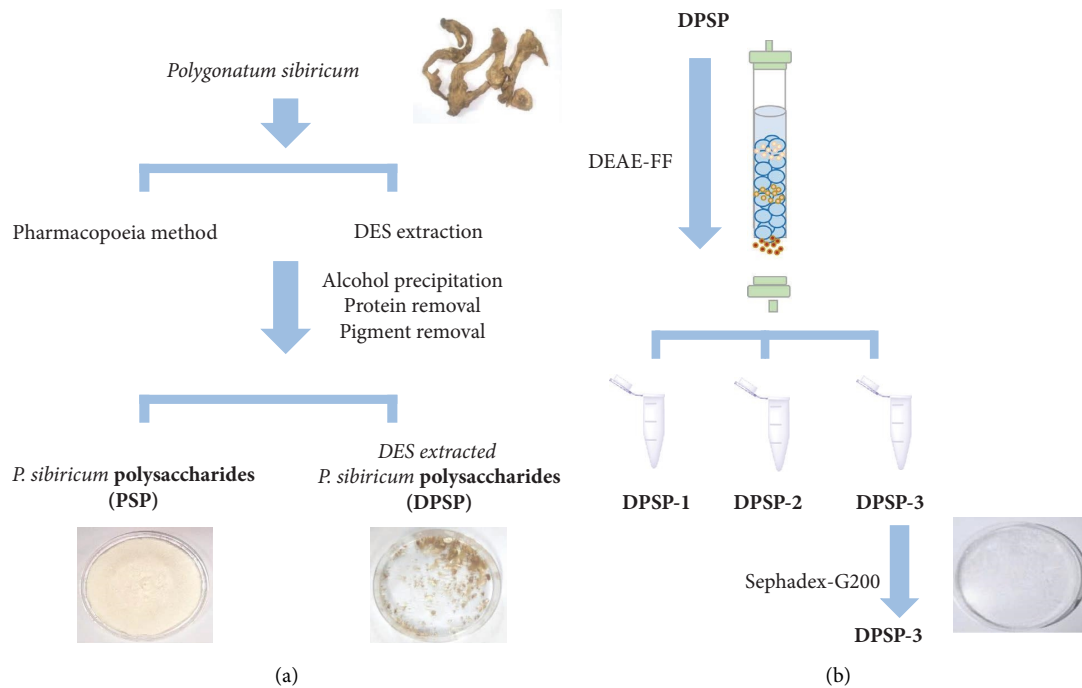


FIGURE 1: Preparation and purification of polysaccharides from *P. sibiricum*.

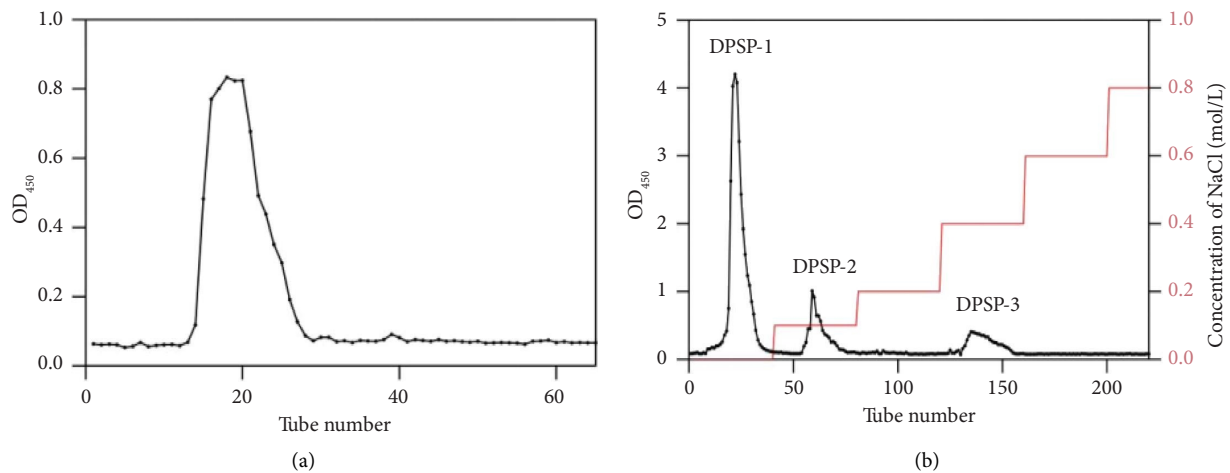


FIGURE 2: Elution chromatographic profile of DPSP on DEAE column (a) and DPSP-3 on Sephadex G-200 column (b).

(Agilent 1206 Series), equipped with a chromatographic column Agilent GPC/SEC PL aquagel-OH MIXED-H column (300 mm × 7.5 mm). The mobile phase was ultrapure water with a flow rate of 1.0 mL/min, and column temperature was set at (30 ± 0.5)°C. The molecular weight was determined by a standard curve of known molecular weights (dextran 6.2, 10, 48.8, 70, 200, and 736 kDa).

**2.3.2. Monosaccharide Composition Determination.** 3.0 mg of polysaccharides was hydrolyzed with TFA (2 mol/L) at 120°C for 4 h and then blow-dried with nitrogen. Subsequently, the dried hydrolyzed samples were dissolved in 3.0 mL ultrapure water. The 250 μL sample hydrolysate

was dissolved in 500 μL 0.4 mol/L 1-phenyl-3-methyl-5-pyrazolone (PMP) methanol solvent and 250 μL 0.6 mol/L NaOH solution for derivatization at 70°C for 1 h. The solution was cooled down to room temperature before the addition of 500 μL 0.3 mol/L HCl and 1 mL chloroform. Subsequently, the solution was centrifuged at 3000 rpm for 10 min and carefully took supernatant. The solution was extracted three times. Finally, the Shimadzu LC-20AD system (Shimadzu Research Laboratory Co. Ltd, Kyoto, Japan) coupled with Welch Xtimate C18 (200 mm × 4.6 mm, 5 μm, Ingersoll Rand Inc., Fürstenfeldbruck, Germany) was utilized for analyzing PMP derivatives. KH<sub>2</sub>PO<sub>4</sub>/acetonitrile was used as the mobile phase. The flow rate was set at 1.0 mL/min at 30°C.

**2.3.3. Conformational Features Determination.** Fourier transform infrared (FT-IR) spectra analysis: the infrared spectrum was determined using the Nicolet iN10 microscope infrared spectrometer (Thermo Fisher Technology Co., Shanghai, China). 100 mg of KBr was added to 1 mg of polysaccharides and then ground and pressed. Infrared full-wavelength mode spectral scanning was performed in the frequency range of 4000 to 400  $\text{cm}^{-1}$ .

Triple-helix structure analysis: Congo red solution (2 mL, 80  $\mu\text{mol/L}$ ) and polysaccharides solution (2 mL, 2.5 mg/mL) were mixed at a ratio of 1:1. NaOH solution was added to make the final concentration of NaOH with 0.0–0.5 mol/L. The maximum absorption wavelength was measured by using the UV-vis spectrophotometer (TU-1810PU, Beijing Purkinje General instrumental factory, Beijing, China).

**2.3.4. Scanning Electron Microscopy (SEM) Observation.** Scanning electron microscopy (SEM) (Carl Zeiss AG, Oberkochen, Baden-Wurttemberg, Germany) was used to observe the polysaccharides microstructure. The polysaccharides were evenly coated on the carrier platform and before being coated with a thin layer of gold using a sputter coater (MC1000, Hitachi Limited, Tokyo, Japan). The gold-sprayed sample was placed in a scanning electron microscope, and the morphology was observed at 500x 1000x 2000x magnification.

#### 2.4. Immunomodulatory Activity of the PSP and DPSP-3 in RAW 264.7 Cells

**2.4.1. Cell Culture.** The RAW 264.7 cells were cultured in a high-sugar DMEM medium containing 10% fetal bovine serum (FBS), 0.1 IU/mL insulin, and 1% dual antibiotics (penicillin and streptomycin) at 37°C with 5%  $\text{CO}_2$ .

**2.4.2. Cell Viability Assay.** The cell viability was assessed using a CCK-8 assay kit (CCK-8; Biosharp, Hefei, Anhui, China) according to the instructions of the manufacturer. The cells were incubated in 96-well plates at a density of  $2 \times 10^4$  cells/well. They were then treated with different PSP and DPSP-3 concentrations (0, 100, 200, 400, 800, and 1000  $\mu\text{g/mL}$ ) in the incubator for 24 h. The supernatant was discarded. The sample was added 100  $\mu\text{L}$  DMEM culture medium (without serum) and 10  $\mu\text{L}$  CCK-8 solution, and then incubated for 15 min. The absorbance at 450 nm was measured using a microplate reader (Multiskan FC, Thermo Fisher Scientific, USA).

**2.4.3. Phagocytosis Assay.** The effects of PSP and DPSP-3 on the phagocytosis of RAW 264.7 cells were measured by using the neutral red assay kit [23]. RAW 264.7 cells ( $1 \times 10^5$  cells/mL) were loaded into 96-well plates. After 24 h incubation, DEME culture medium, LPS (25  $\mu\text{g/mL}$ ), or different concentrations of 200, 400, and 800  $\mu\text{g/mL}$ , PSP and DPSP-3 solutions were pipetted into each well for another 24 h incubation. The medium was carefully removed, and 100  $\mu\text{L}$  of 0.1% neutral red was added into each well and incubated for 1 h. After washing three times with PBS, each of the wells was

loaded with 100  $\mu\text{L}$  of cell lysis solution (glacial acetic acid: ethanol = 1 : 1). The cell culture plate was statically placed at 4°C overnight. The absorbance at 540 nm was measured using a microplate reader (Multiskan FC, Thermo Fisher Scientific, USA).

**2.4.4. Determination of ROS, NO, TNF- $\alpha$ , and IL-6.** ROS production by RAW 264.7 cells was measured using 2,7-dichlorofluorescein diacetate (DCFH-DA). Macrophages ( $1 \times 10^6$  cells/mL) were seeded into 96-well plates for 24 h. Then, cells were incubated in the DMEM culture medium with 200, 400, and 800  $\mu\text{g/mL}$  PSP, DPSP-3 solution, or LPS (25  $\mu\text{g/mL}$ ). After 24 h incubation, all culture medium was carefully removed, followed by the addition of 100  $\mu\text{L}$  DCFH-DA (10  $\mu\text{M}$ ) dissolved in the serum-free medium for 30 min at 37°C. Then, the supernatant was removed, and the cells were washed three times with PBS. Fluorescence intensity was immediately detected at 485 nm excitation and at 525 nm emission using a microplate reader (Multiskan FC, Thermo Fisher Scientific, USA).

The RAW264.7 cells ( $1 \times 10^5$  cells/mL) were pipetted into 24-well plates, which were then incubated with 200, 400, and 800  $\mu\text{g/mL}$  PSP, DPSP-3 solutions, or LPS (25  $\mu\text{g/mL}$ ). The samples were centrifuged for separation (2,000 rpm, 10 min), and the supernatant was collected for the subsequent experiments. The release of NO was determined by using the NO determination kit (Jiancheng bioengineering institute, Nanjing, China) according to manufacturer's instruction. The release of TNF- $\alpha$  and IL-6 was determined by using commercial ELISA kits (Mlbio, Shanghai, China) according to the manufacturer's instructions.

**2.5. Statistical Analysis.** All experimental data were expressed as means  $\pm$  standard deviation (SD). Statistical calculations and graphing were performed using GraphPad Prism 8.0.2. SPSS 20.0 was used to evaluate statistical significance, and  $p < 0.05$  was considered statistically significant.

### 3. Results and Discussion

**3.1. Isolation and Purification.** The yields of PSP and DPSP were (10.21  $\pm$  0.50)% and (15.62  $\pm$  0.71)% (w/w), respectively, and the yield of DPSP was 1.53 times that of PSP. Wang found that the optimal extract rates of flavonoids from *Moringa oleifera* leaves by DES were 1.17 times and 1.42 times that of ethanol extraction and water extraction, respectively, and flavonoids by DES improved antioxidant, antibacterial, and antitumor activities [24]. Wu extracted acidic polysaccharides from lotus leaves with DES, and the results showed that the maximum yield (5.38%) was 1.67 times that of polysaccharides prepared with the pharmacopoeia method [25]. These results were consistent with this study.

DPSP solution was eluted by DEAE-Sepharose Fast Flow column, and three peaks were obtained when concentration of NaCl increased to 0.4 mol/L in the elation, as illustrated in Figure 2(a). They were named as DPSP-1, DPSP-2, and DPSP-3. DPSP-3 purified by the Sephadex G-200 column had a single symmetric peak (Figure 2(b)).

### 3.2. Structural Characterization

**3.2.1. Molecular Weight Analysis.** Molecular weight affected the absorption of polysaccharides *in vivo* by affecting the physicochemical properties of polysaccharides such as solubility and viscosity [26]. Some studies showed the high molecular weight usually inhibits its absorption, yet low molecular weight compounds were unable to form active triple-helix conformation [27]. As shown in Figures 3(a) and 3(b), PSP and DPSP contained more than one fraction due to the presence of multiple peaks in the chromatogram. The molecular weight of PSP ranged from  $9.4 \times 10^7$  to  $6.9 \times 10^3$  Da, and DPSP had four main peaks which were  $4.1 \times 10^7$ ,  $7.7 \times 10^5$ ,  $7.9 \times 10^3$ , and  $1.4 \times 10^3$  Da, respectively. Molecular weight analysis of PSP, DPSP, and DPSP-3 showed that the DES extraction method could degrade polysaccharides. As shown in Figure 3(c), DPSP-3 showed a single symmetric peak ( $3.2 \times 10^6$  Da) with a higher molecular weight. Wang found that the immunological activity of *P. sibiricum* polysaccharides was related to the molecular weight and main composition of monosaccharide, the immunological activity of high molecular weight polysaccharides was higher than that of low molecular weight polysaccharides, and the higher ratio of Gal and Rha significantly improved the phagocytosis in RAW264.7 cells [20].

**3.2.2. Monosaccharide Composition Analysis.** Different monosaccharide compositions have an important influence on the immunomodulatory activity of polysaccharides. The study showed that the more complex the monosaccharide composition was, the better the biological activity of polysaccharides displayed [28]. *Helicteres angustifolia* L. polysaccharides with high ratios of arabinose, galactose, xylose, and uronic acid significantly enhanced the proliferation of macrophages and stimulated the macrophages phagocytic capacity, as well as induced NO and immunomodulatory cytokines [29]. *Passiflora foetida* polysaccharides with high content of mannose (48.83%) could promote the release of NO, TNF- $\alpha$ , and IL-6 from macrophages [30], and the high content of mannose could contribute to the mild immunostimulatory activity [28]. The monosaccharide composition of PSP, DPSP, and DPSP-3 is shown in Figure 4. These polysaccharides consisted of mannose, rhamnose, glucose, galactose, arabinose, and a small number of glucuronic acid and galacturonic acid. Results showed that DPSP and DPSP-3 had more mannose, rhamnose, galactose, and galacturonic acid, yet less glucose and glucuronic acid. After purification, the galactose content of DPSP-3 was 65.75%, which was 13.45 times that of the PSP. The mannose content of DPSP-3 was 19.76%, which was 1.65 times that of the PSP. The rhamnose content of DPSP-3 was 4.48%, which was 16 times that of the PSP.

**3.2.3. Conformational Analysis.** Figure 5(a) showed the FT-IR spectra of PSP, DPSP, and DPSP-3. The absorption peak at about  $3330 \text{ cm}^{-1}$  corresponds to O-H stretching vibration absorption [31]. The absorption peak at  $2926 \text{ cm}^{-1}$

corresponds to C-H stretching vibration absorption [32], while peak at  $1371 \text{ cm}^{-1}$  corresponds to C-H bending vibration absorption. These three absorption peaks are characteristic peaks of polysaccharides. The absorption peak at  $1631 \text{ cm}^{-1}$  corresponds to C=O bending vibration [33]. The absorption peak at  $1015 \text{ cm}^{-1}$  corresponds to characteristic peaks of C-O-C of glucopyranose, which indicates that the three polysaccharides all contain pyranoside bonds [34]. Meanwhile, absorption peak at about  $889 \text{ cm}^{-1}$  corresponds to  $\beta$ -glucosidic bonds [35], and DPSP-3 was higher than the other two polysaccharides, indicating that it contained more  $\beta$ -glucoside bonds. Some studies showed that polysaccharides with  $\beta$  configuration had higher activity [26].

As seen from Figure 5(b), after the maximum absorption, wavelengths showed obvious red-shift phenomenon, while with the increase of NaOH concentration,  $\lambda_{\text{max}}$  did not decrease significantly. These results indicated that three polysaccharides had typical triple-helix conformation and were relatively stable at the concentration of 0–0.4 mol/L NaOH. Studies showed that polysaccharides changed to single-flexible chains, resulting in decreasing bioactivity [36]. Previous research showed that the triple-helix structure of *P. sibiricum* polysaccharides was stable at the concentration of 0–0.4 mol/L NaOH [37], suggesting that DPSP might have higher and more stable biological activity.

**3.2.4. SEM Analysis.** The SEM images of PSP, DPSP, and DPSP-3 were shown in Figure 6. PSP presented a flat, flaky, and rough surface. Although DPSP also had a flake and rough morphology, it also had a lot of independent spherical convex. DPSP-3 presented a curly shape and had smooth, porous, and lamellar surface with a few spherical edges. Research showed that acid sugar with large molecules had negatively charged, which resulted in increasing repulsive force between the molecules [38]. The smooth surface of polysaccharides probably had negative effect on the rehydration performance to reduce its solubility, which accounted for the lower solubility of some polysaccharides [39]. Therefore, compared with the flat and flaky structure, the curly structure of DPSP-3 predicted better biological activity. It indicated that different extraction and purification methods changed the morphological characteristics of polysaccharides.

### 3.3. Immunomodulatory Activity

**3.3.1. The Effects on the Cell Viability of RAW264.7 Cells.** Figure 7(a) showed the effects of PSP and DPSP-3 on the cell viability of RAW264.7. They showed no significant toxicity to RAW 264.7 cells at 100–1000  $\mu\text{g/mL}$ . By contrast, in the concentration range of 200–1000  $\mu\text{g/mL}$ , although two polysaccharides promoted cellular proliferation, concentration of 1000  $\mu\text{g/mL}$  showed the lower proliferation effect. Therefore, polysaccharides concentration at 200, 400, and 800  $\mu\text{g/mL}$  was chosen for the subsequent immunomodulatory activity experiments.

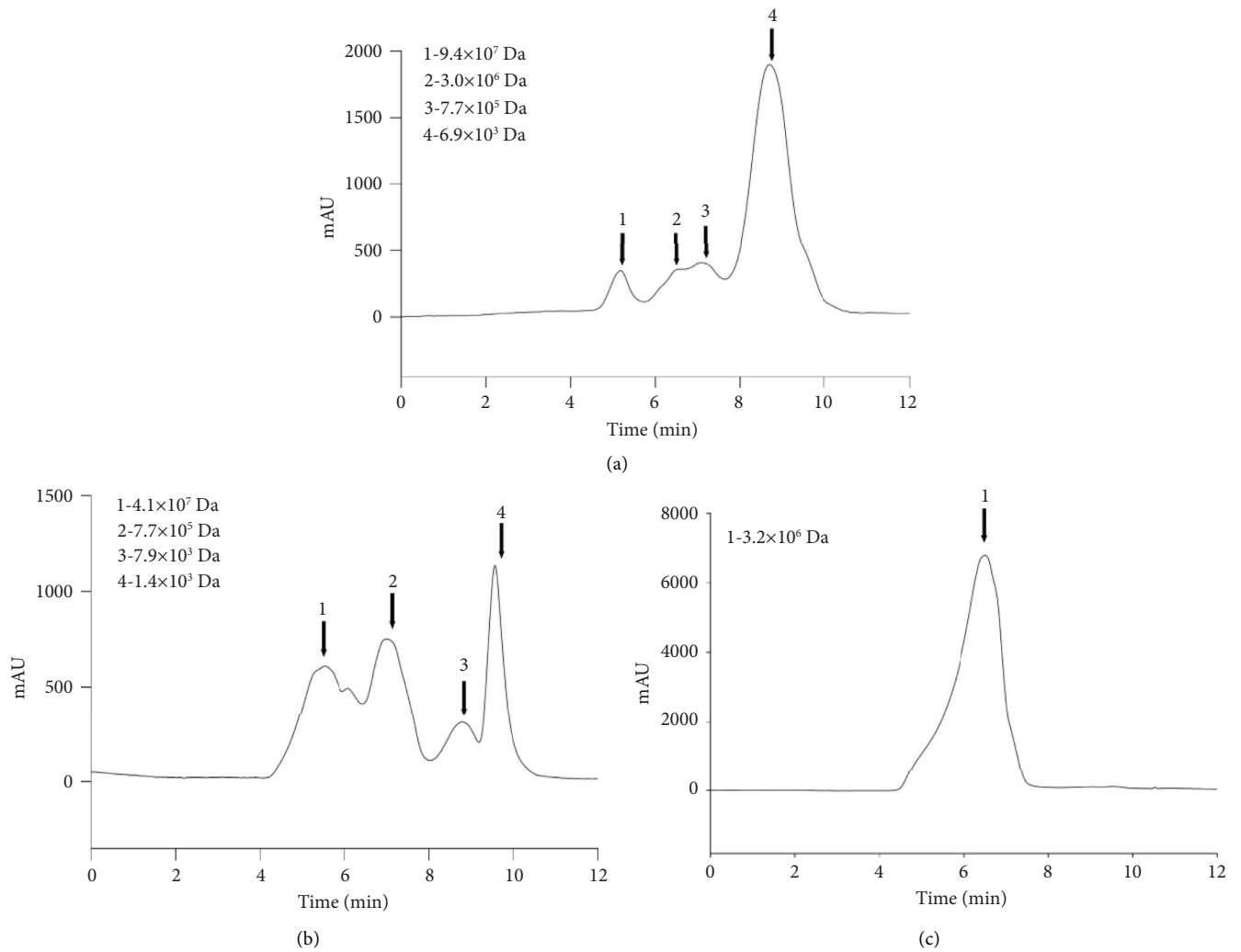


FIGURE 3: The GPC diagram of PSP (a), DPSP (b), and (c) DPSP-3.

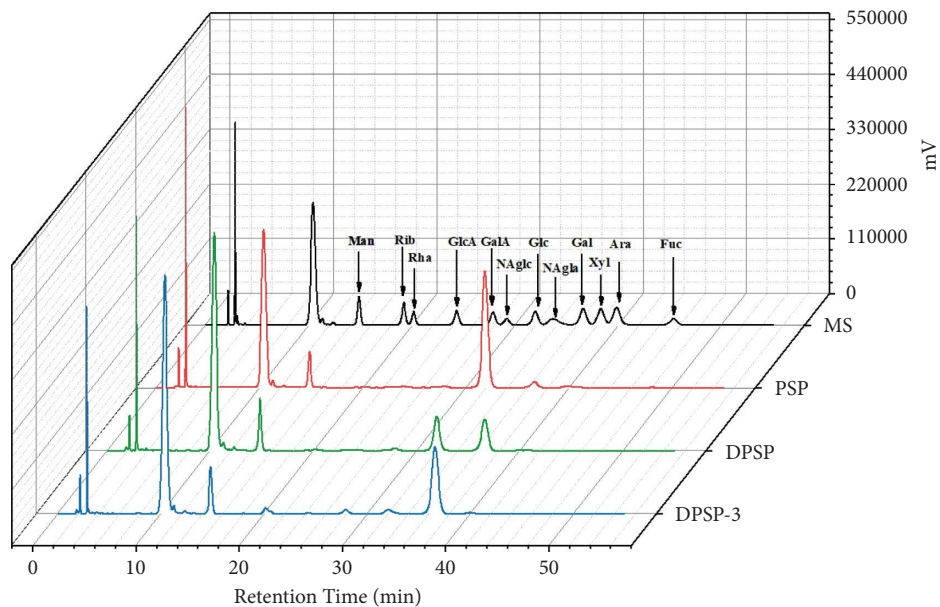


FIGURE 4: Chromatograms of PSP, DPSP, and DPSP-3. Ara, arabinose; Fuc, fucose; Gal, galactose; Glc, glucose; GlcA, glucuronic acid; GalA, galacturonic acid; Man, mannose; NAgal, N-acetyl-d-galactosamine; NAglc, N-acetyl-d-glucosamine; Rib, ribose; Rha, rhamnose; Xyl, xylose; the different lowercase letters in different columns indicate significant differences at  $p < 0.05$ .

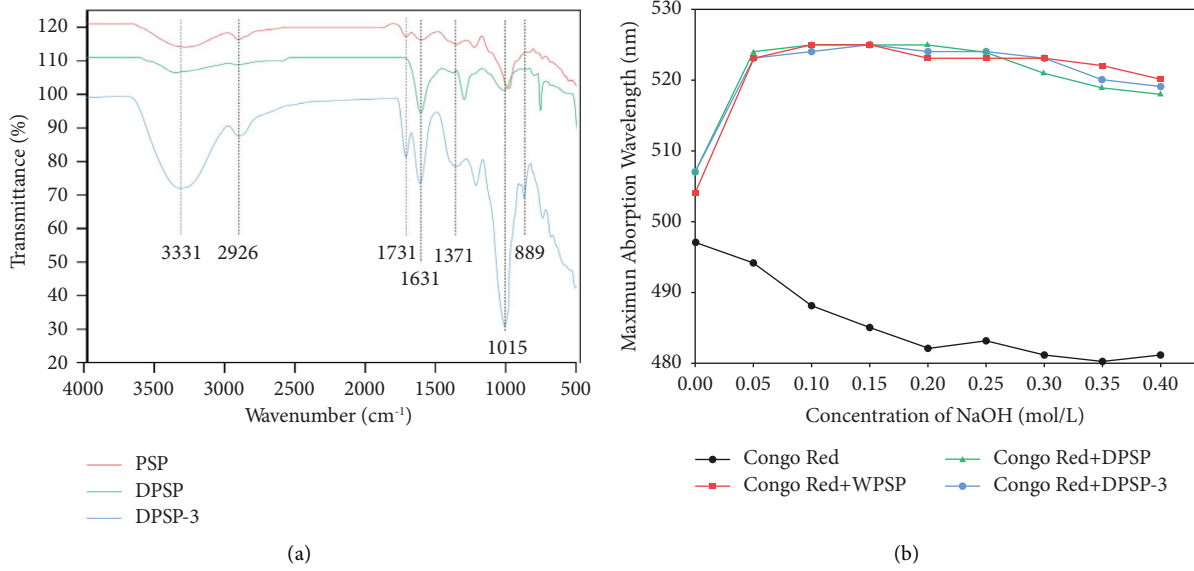


FIGURE 5: Conformational features: the FT-IR spectra of PSP, DPSP, and DPSP-3 (a) and the triple-helix conformation analysis of PSP, DPSP, and DPSP-3 (b).

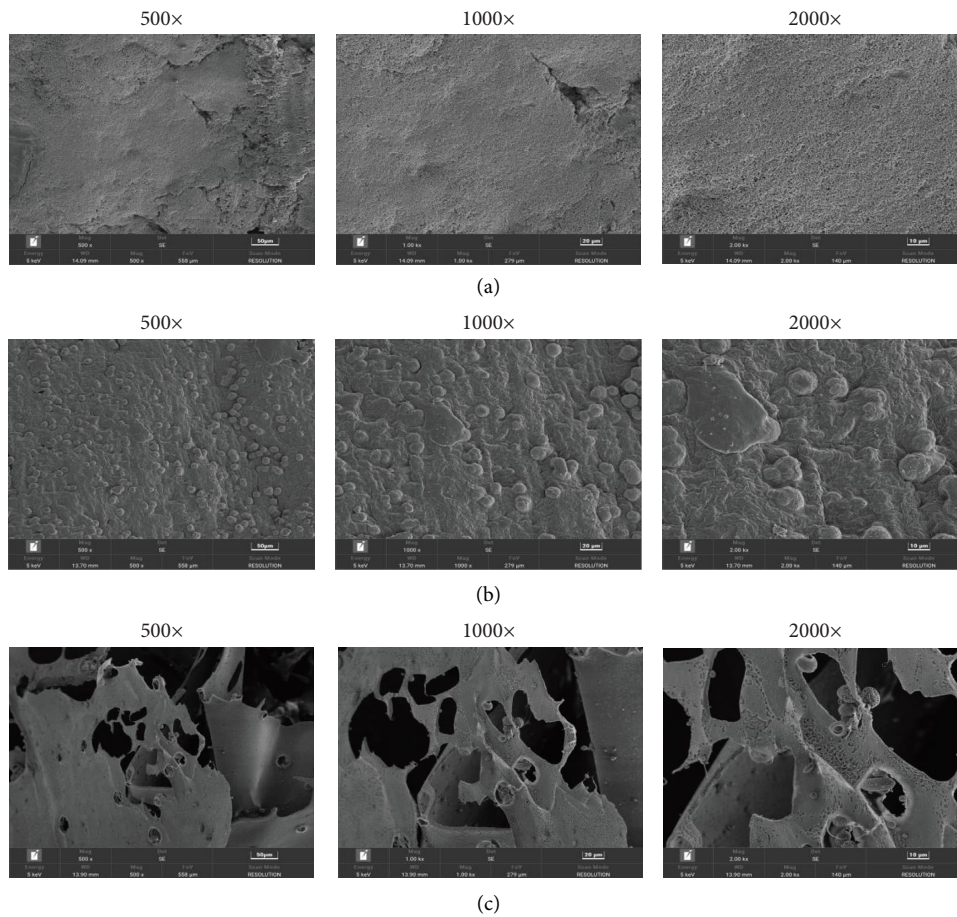


FIGURE 6: SEM spectra of PSP (a), DPSP (b), and (c) DPSP-3.

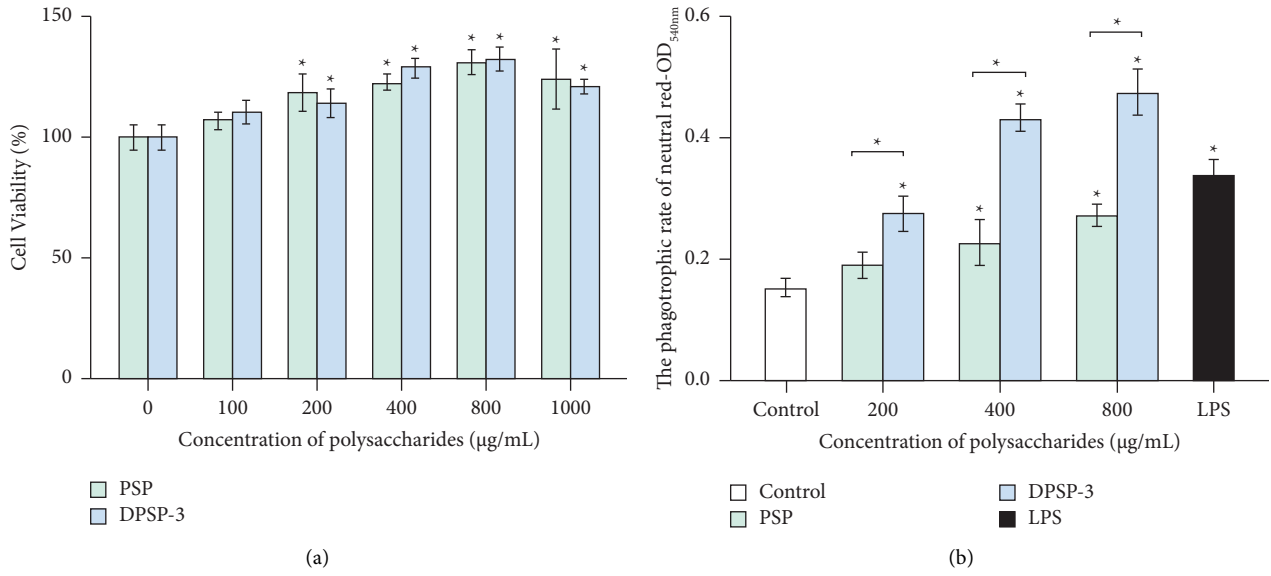


FIGURE 7: Effects of PSP and DPSP-3 at different concentrations on RAW 264.7 cells: cell viability (a) and phagocytosis activity (b). Significant differences with the blank group or the control group are indicated as \* $p < 0.05$ .

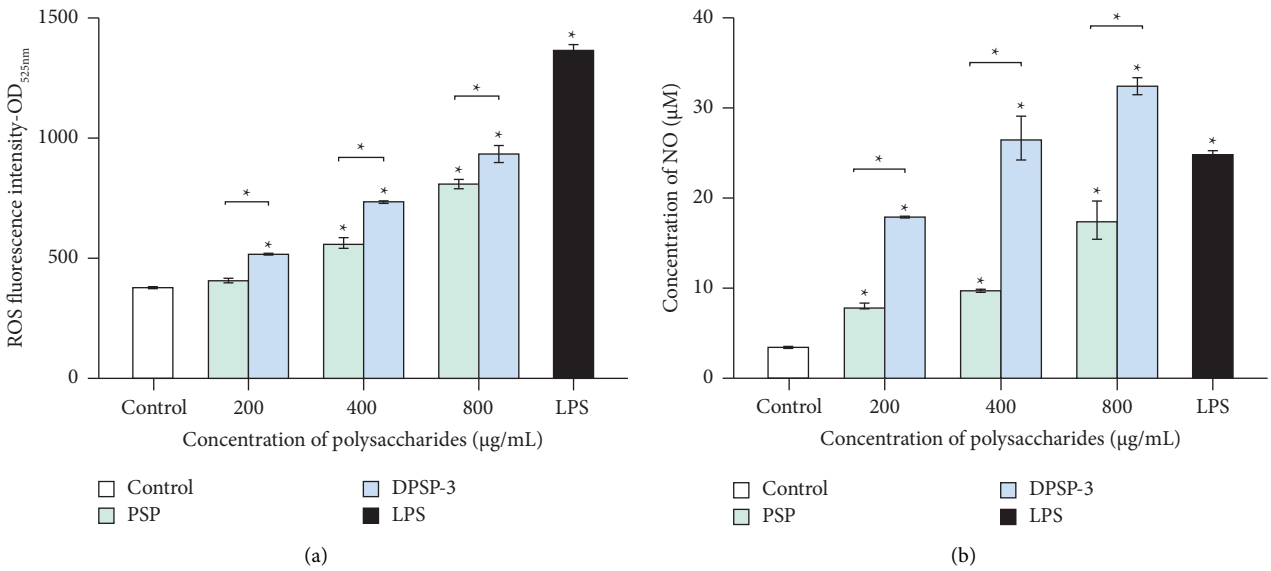


FIGURE 8: Continued.



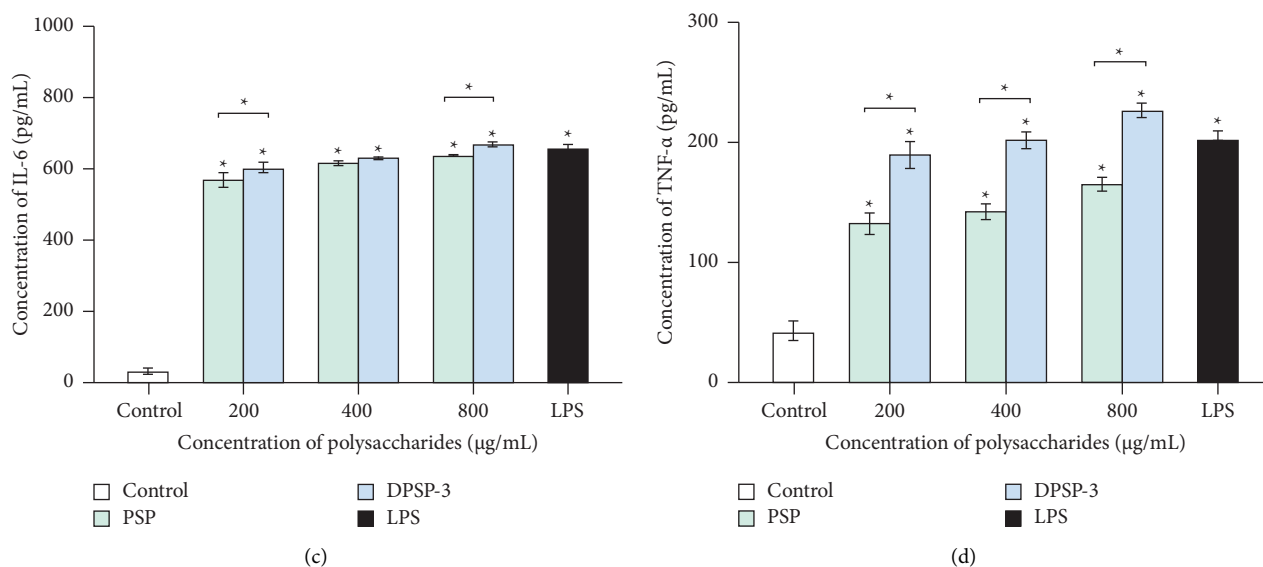


FIGURE 8: Effects of PSP and DPSP-3 at different concentrations on RAW 264.7 cells: The release level of ROS (a), NO (b), IL-6 (c), and TNF- $\alpha$  (d). Significant differences with the control group are indicated as \* $p < 0.05$ .

**3.3.2. The Effects on the Phagotrophic Ability of RAW264.7 Cells.** Phagocytosis of macrophages is the most basic regulatory mechanism in the immune response and one of the main characterizations of its immunity activation. Phagocytosis can be divided into three steps: recognition of foreign substances, formation of phagosomes, and maturation of phagosomes [40]. The phagocytosis of macrophages can reflect the activation degree of macrophages, and the phagocytosis of neutral red can simply and quickly reflect the phagocytosis of macrophages. As shown in Figure 7(b), the phagocytosis ability of RAW264.7 cells significantly enhanced dose-dependently. DPSP-3 was significantly higher than PSP in three concentrations. At high concentration (800  $\mu\text{g/mL}$ ), the PSP group of phagotrophic rate was 1.78 times that of the control group, the DPSP-3 group of phagotrophic rate was 3.09 times that of the control group. This might be attributed to the fact that the immunomodulatory activity of the polysaccharides was related to the molecular weight and the major monosaccharide composition. Meanwhile, the higher Gal and Rha content in DPSP-3 had an important effect on the improvement of the phagocytosis capacity of RAW264.7 cells [28].

**3.3.3. The Effects on the Release of NO, ROS, IL-6, and TNF- $\alpha$  of RAW264.7 Cells.** NO and ROS play an important role in the immune function of macrophages and can be used as intracellular messengers to activate inflammatory signaling pathways and mediate biological immune responses [41]. The release of NO and ROS in RAW.264.7 cells treated with PSP and DPSP-3 was increased, except at low concentration (200  $\mu\text{g/mL}$ ). As shown in Figures 8(a) and 8(b), the ROS fluorescence intensity of the LPS, PSP, and DPSP-3 groups was higher than that of the control group. With the increase of polysaccharides concentration, the release of NO and ROS increased in RAW.264.7 cells. In detail, the release of ROS

was significantly increased by 13.8% and 46.6% at 800  $\mu\text{g/mL}$  of PSP and DPSP-3, respectively. Previous studies reported that glucose residues in polysaccharides stimulated ROS release in RAW264.7 cells through Toll-like receptor 4 (TLR4) [42]. ROS is not only a landmark of cell activation but also an intermediate in the ROS-cSrc-NF $\kappa$ B signaling cascade in RAW264.7 cells [43].

Macrophages are one of the most important immune cells, and the activated macrophages can eliminate pathogens or tumor cells by phagocytosis or secretion of pro-inflammatory factors [21, 44]. As can be seen from Figures 8(c) and 8(d), PSP and DPSP-3 significantly stimulated the release of IL-6 and TNF- $\alpha$  in RAW264.7 cells at 200–800  $\mu\text{g/mL}$ . The release of IL-6 was measured as (567.28  $\pm$  20.44) and (602.16  $\pm$  16.66) pg/mL at 200  $\mu\text{g/mL}$ , respectively, which were 19.67 times and 20.88 times that of the control group. TNF- $\alpha$  showed a significant dose-dependent relationship with PSP and DPSP-3. At 800  $\mu\text{g/mL}$ , the release of TNF- $\alpha$  was (165.71  $\pm$  6.01) and (227.16  $\pm$  5.29) pg/mL, respectively, which were 3.80 times and 6.35 times that of the control group. Compared with PSP, DPSP-3 could significantly improve the release of TNF- $\alpha$  by about 37%.

## 4. Conclusion

In this study, we isolated and purified polysaccharides from *P. sibiricum* and analyzed their structural characterization and immunomodulatory activity in RAW264.7 cells. The yield of DPSP was (15.62  $\pm$  0.71)%, and its yield was 1.53 times that of PSP. DPSP-3 purified from DPSP at 0.04 M NaCl showed molecular weight of  $3.2 \times 10^6$  Da, and the content of galactose, mannose, and rhamnose was 13.45, 1.65, and 16.00 times that of PSP, respectively. Both PSP and DPSP-3 significantly improved phagotrophic capacity and increased the release of ROS, NO, IL-6, and TNF- $\alpha$  in

RAW264.7 cells. Meanwhile, DPSP-3 exhibited better immunomodulatory activity, which might be related to the higher content of mannans, galactose,  $\beta$ -glucosidic, bonds, and triple-helix structure in DPSP-3. Based on the speculation of the relationship between the structure and immunomodulatory activity of *P. sibiricum* polysaccharides in this study, the immune-related receptors and pathways can be studied in the future. In general, DES can not only improve the yield of polysaccharides but also change the structure and activity of polysaccharides. However, the principle of changing polysaccharides structure and the mechanism of enhancing polysaccharides activity are not clear. These questions need to be further explored. This study developed an efficient method for preparing polysaccharides from *P. sibiricum* utilizing DES. The results showed that DES was an efficient solvent for polysaccharides extraction, and DPSP-3 could be used as potential immunomodulatory agents in the fields of health food industry.

### Data Availability

The data used to support the findings of this study are available from the corresponding author upon request.

### Conflicts of Interest

The authors declare that there are no conflicts of interest.

### Acknowledgments

This work was supported by National Key R&D Program of China (Grant No. 2021YFD2100200/2021YFD2100204) and Guizhou Province Science and Technology Plan Project (Grant No. 20204Y070).

### References

- [1] Y. Wang, F. Xu, J. Cheng et al., "Natural deep eutectic solvent-assisted extraction, structural characterization, and immunomodulatory activity of polysaccharides from *paecilomyces hepiali*," *Molecules*, vol. 27, no. 22, p. 8020, 2022.
- [2] H. Zhang, J. Lang, P. Lan, H. Yang, J. Lu, and Z. Wang, "Study on the dissolution mechanism of cellulose by ChCl-based deep eutectic solvents," *Materials*, vol. 13, no. 2, p. 278, 2020.
- [3] H. Zhang, F. Hao, Z. Yao, J. Zhu, X. Jing, and X. Wang, "Efficient extraction of flavonoids from *Polygonatum sibiricum* using a deep eutectic solvent as a green extraction solvent," *Microchemical Journal*, vol. 175, p. 107168, 2022.
- [4] T. El Achkar, H. Greige-Gerges, and S. Fourmentin, "Basics and properties of deep eutectic solvents: a review," *Environmental Chemistry Letters*, vol. 19, no. 4, pp. 3397–3408, 2021.
- [5] H. Bowen, R. Durrani, A. Delavault et al., "Application of deep eutectic solvents in protein extraction and purification," *Frontiers of Chemistry*, vol. 10, Article ID 912411, 2022.
- [6] X. Shang, D. Chu, J. Zhang, Y. Zheng, and Y. Li, "Microwave-assisted extraction, partial purification and biological activity in vitro of polysaccharides from bladder-wrack (*Fucus vesiculosus*) by using deep eutectic solvents," *Separation and Purification Technology*, vol. 259, Article ID 118169, 2021.
- [7] M. Zdanowicz, K. Wilpiszewska, and T. Szychaj, "Deep eutectic solvents for polysaccharides processing. A review," *Carbohydrate Polymers*, vol. 200, pp. 361–380, 2018.
- [8] W. Zhang, S. Cheng, X. Zhai et al., "Green and efficient extraction of polysaccharides from *poria cocos* F.A. Wolf by deep eutectic solvent," *Natural Product Communications*, vol. 15, no. 2, Article ID 1934578X1990070, 2020.
- [9] X. Zou, J. Xiao, J. Chi et al., "Physicochemical properties and prebiotic activities of polysaccharides from *Zizyphus jujube* based on different extraction techniques," *International Journal of Biological Macromolecules*, vol. 223, pp. 663–672, 2022.
- [10] M. Sui, S. Feng, G. Liu, B. Chen, Z. Li, and P. Shao, "Deep eutectic solvent on extraction of flavonoid glycosides from *Dendrobium officinale* and rapid identification with UPLC-triple-TOF/MS," *Food Chemistry*, vol. 401, Article ID 134054, 2023.
- [11] O. A. Olalere and C. Y. Gan, "Extractability of defatted wheat germ protein and their functionalities in a deep eutectic solvent (DES)-Microwave extraction approach compared to conventional processing," *Sustainable Chemistry and Pharmacy*, vol. 32, Article ID 101002, 2023.
- [12] K. Gautam and D. Datta, "Recovery of nicotinic acid (Niacin) using hydrophobic deep eutectic solvent: ultrasonication facilitated extraction," *Chemical Data Collections*, vol. 41, Article ID 100934, 2022.
- [13] X. Zong, D. Xu, J. Yin, S. Nie, and M. Xie, "A review on extraction, purification, structural characteristics and bioactivities of polysaccharides from *Polygonatum odoratum* (mill) druce," *Bioactive Carbohydrates and Dietary Fibre*, vol. 27, 2022.
- [14] S. Xu, J. Bi, W. Jin, B. Fan, and C. Qian, "Determination of polysaccharides composition in *Polygonatum sibiricum* and *Polygonatum odoratum* by HPLC-FLD with pre-column derivatization," *Heliyon*, vol. 8, no. 5, Article ID e09363, 2022.
- [15] J. Bi, C. Zhao, W. Jin, Q. Chen, B. Fan, and C. Qian, "Study on pharmacokinetics and tissue distribution of *Polygonatum sibiricum* polysaccharide in rats by fluorescence labeling," *International Journal of Biological Macromolecules*, vol. 215, pp. 541–549, 2022.
- [16] G. Luo, J. Lin, W. Cheng, Z. Liu, T. Yu, and B. Yang, "UHPLC-Q-Orbitrap-MS-Based metabolomics reveals chemical variations of two types of rhizomes of *Polygonatum sibiricum*," *Molecules*, vol. 27, no. 15, p. 4685, 2022.
- [17] J. Su, Y. J. Wang, M. Q. Yan et al., "The beneficial effects of *Polygonatum sibiricum* Red. superfine powder on metabolic hypertensive rats via gut-derived LPS/TLR4 pathway inhibition," *Phytomedicine*, vol. 106, Article ID 154404, 2022.
- [18] S. Zheng, "Protective effect of *Polygonatum sibiricum* Polysaccharide on D-galactose-induced aging rats model," *Scientific Reports*, vol. 10, no. 1, p. 2246, 2020.
- [19] H. Zhang, X. T. Cai, Q. H. Tian et al., "Microwave-assisted degradation of polysaccharide from *Polygonatum sibiricum* and antioxidant activity," *Journal of Food Science*, vol. 84, no. 4, pp. 754–761, 2019.
- [20] Y. J. Wang, N. Liu, X. Xue, Q. Li, D. Q. Sun, and Z. X. Zhao, "Purification, structural characterization and in vivo immunoregulatory activity of a novel polysaccharide from *Polygonatum sibiricum*," *International Journal of Biological Macromolecules*, vol. 160, pp. 688–694, 2020.
- [21] Z. Wu, D. Wang, C. X. Liu et al., "Macrophage immunity promotion effect of polysaccharide LGP-1 from Guapian tea via PI3K/AKT and NF- $\kappa$ B signaling pathway," *Journal of Functional Foods*, vol. 89, Article ID 104946, 2022.

- [22] S. Yu, X. Dong, R. Ma, H. Ji, J. Yu, and A. Liu, "Characterization of a polysaccharide from *Polygala tenuifolia* willd. with immune activity via activation MAPKs pathway," *Bio-organic Chemistry*, vol. 130, Article ID 106214, 2023.
- [23] F. F. Wu, C. H. Zhou, D. D. Zhou, S. Y. Ou, X. A. Zhang, and H. H. Huang, "Structure characterization of a novel polysaccharide from *Hericium erinaceus* fruiting bodies and its immunomodulatory activities," *Food & Function*, vol. 9, no. 1, pp. 294–306, 2018.
- [24] Y. Wang, C. Peng, Y. Zhang et al., "Optimization, identification and bioactivity of flavonoids extracted from *Moringa oleifera* leaves by deep eutectic solvent," *Food Bioscience*, vol. 47, Article ID 101687, 2022.
- [25] D. T. Wu, K. L. Feng, L. Huang, R. Y. Gan, Y. C. Hu, and L. Zou, "Deep eutectic solvent-assisted extraction, partially structural characterization, and bioactivities of acidic polysaccharides from Lotus leaves," *Foods*, vol. 10, p. 2330, 2021.
- [26] B. Wang, L. L. Yan, S. C. Guo et al., "Structural elucidation, modification, and structure-activity relationship of polysaccharides in Chinese herbs: a review," *Frontiers in Nutrition*, vol. 9, Article ID 908175, 2022.
- [27] C. Wang, W. W. Li, Z. Q. Chen et al., "Effects of simulated gastrointestinal digestion in vitro on the chemical properties, antioxidant activity, alpha-amylase and alpha-glucosidase inhibitory activity of polysaccharides from *Inonotus obliquus*," *Food Research International*, vol. 103, pp. 280–288, 2018.
- [28] Y. He, L. Li, H. Chang et al., "Research progress on extraction, purification, structure and biological activity of *Dendrobium officinale* polysaccharides," *Frontiers in Nutrition*, vol. 9, Article ID 965073, 2022.
- [29] S. Sun, K. J. Li, L. Xiao, Z. F. Lei, and Z. Y. Zhang, "Characterization of polysaccharide from *Helicteres angustifolia* L. and its immunomodulatory activities on macrophages RAW264.7," *Biomedicine & Pharmacotherapy*, vol. 109, pp. 262–270, 2019.
- [30] Y. Song, M. Q. Zhu, H. L. Hao et al., "Structure characterization of a novel polysaccharide from Chinese wild fruits (*Passiflora foetida*) and its immune-enhancing activity," *International Journal of Biological Macromolecules*, vol. 136, pp. 324–331, 2019.
- [31] Y. L. Ren, G. Q. Zheng, L. J. You et al., "Structural characterization and macrophage immunomodulatory activity of a polysaccharide isolated from *Gracilaria lemaneiformis*," *Journal of Functional Foods*, vol. 33, pp. 286–296, 2017.
- [32] G. T. Cui, W. X. Zhang, Q. J. Wang et al., "Extraction optimization, characterization and immunity activity of polysaccharides from *Fructus Jujubae*," *Carbohydrate Polymers*, vol. 111, pp. 245–255, 2014.
- [33] Y. W. Liu, K. M. Mao, N. Zhang et al., "Structural characterization and immunomodulatory effects of extracellular polysaccharide from *Lactobacillus paracasei* VL8 obtained by gradient ethanol precipitation," *Journal of Food Science*, vol. 87, no. 5, pp. 2034–2047, 2022.
- [34] X. C. Liu, Z. Y. Zhu, Y. L. Tang et al., "Structural properties of polysaccharides from cultivated fruit bodies and mycelium of *Cordyceps militaris*," *Carbohydrate Polymers*, vol. 142, pp. 63–72, 2016.
- [35] B. Yang, Q. J. Wu, Y. X. Luo et al., "Japanese grape (*Hovenia dulcis*) polysaccharides: new insight into extraction, characterization, rheological properties, and bioactivities," *International Journal of Biological Macromolecules*, vol. 134, pp. 631–644, 2019.
- [36] Y. Y. Zhang, S. Li, X. H. Wang, L. N. Zhang, and P. C. K. Cheung, "Advances in lentinan: isolation, structure, chain conformation and bioactivities," *Food Hydrocolloids*, vol. 25, no. 2, pp. 196–206, 2011.
- [37] J. B. Bai, J. C. Ge, W. J. Zhang et al., "Physicochemical, morpho-structural, and biological characterization of polysaccharides from three *Polygonatum* spp.," *RSC Advances*, vol. 11, no. 60, pp. 37952–37965, 2021.
- [38] M. S. Riaz Rajoka, H. M. Mehwish, H. Fang et al., "Characterization and anti-tumor activity of exopolysaccharide produced by *Lactobacillus kefir* isolated from Chinese kefir grains," *Journal of Functional Foods*, vol. 63, Article ID 103588, 2019.
- [39] Z. Y. Chen, Y. Zhao, M. K. Zhang et al., "Structural characterization and antioxidant activity of a new polysaccharide from *Bletilla striata* fibrous roots," *Carbohydrate Polymers*, vol. 227, Article ID 115362, 2020.
- [40] H. J. Lee, Y. Woo, T. W. Hahn, Y. M. Jung, and Y. J. Jung, "Formation and maturation of the phagosome: a key mechanism in innate immunity against intracellular bacterial infection," *Microorganisms*, vol. 8, no. 9, p. 1298, 2020.
- [41] Q. Li, T. Zhao, G. H. Mao et al., "A Se-enriched *Grifola frondosa* polysaccharide induces macrophage activation by TLR4-mediated MAPK signaling pathway," *International Journal of Biological Macromolecules*, vol. 238, Article ID 124108, 2023.
- [42] D. D. Wang, W. J. Pan, S. Mehmood, X. D. Cheng, and Y. Chen, "Polysaccharide isolated from *Sarcodon aspratus* induces RAW264.7 activity via TLR4-mediated NF- $\kappa$ B and MAPK signaling pathways," *International Journal of Biological Macromolecules*, vol. 120, pp. 1039–1047, 2018.
- [43] X. L. Cheng, F. Ding, H. Li et al., "Activation of AMPA receptor promotes TNF- $\alpha$  release via the ROS-cSrc-NF $\kappa$ B signaling cascade in RAW264.7 macrophages," *Biochemical and Biophysical Research Communications*, vol. 461, no. 2, pp. 275–280, 2015.
- [44] Y. H. Xie, L. X. Wang, H. Sun et al., "Polysaccharide from alfalfa activates RAW 264.7 macrophages through MAPK and NF- $\kappa$ B signaling pathways," *International Journal of Biological Macromolecules*, vol. 126, pp. 960–968, 2019.